J. Fluid Mech. (1994), *vol.* 278, *pp.* 297–323

On the instabilities of vertical falling liquid films in the presence of surface-active solute

By WEI JI AND FREDRIK SETTERWALL
Department of Chemical Engineering and Technology, Royal Institute of Technology, 100 44 Stockholm, Sweden

(Received 17 November 1993 and in revised form 20 May 1994)

A linear-stability analysis is performed on a vertical falling film with a surface-active solute. It is assumed in the present model that the surfactant is soluble and volatile. In addition to the surface wave mode and the 'wall wave' mode which originate from the gravity-driven flow of the falling film itself, a new mode of instability related to the Marangoni effect induced by surface tension gradients is found for low Reynolds numbers and for moderate- or short-wavelength disturbances. The new mode is thought to be analogous to the thermocapillary instability examined first by Pearson (1958). The Marangoni instability of large-wavelength disturbances, revealed by Goussis & Kelly (1990) in a study of a liquid layer heated from below, may be completely suppressed in the present system by the effect of surface-excess concentration of the surfactant. The influence of the desorption of the solute and of its adsorption at the gas–liquid interface is determined for both the surface wave mode and the new wave mode. Desorption of the surfactant is shown to be responsible for the Marangoni instability of the new mode.

1. Introduction

A stability analysis of a falling film was reported by Li & Ji (1994) for a solution to the Orr–Sommerfeld equation, using a numerical discretization technique. In addition to recovering the previously known surface wave mode of instability, a 'wall wave' mode was found to be unstable for high Reynolds numbers. In the present report, the effect of a surfactant on the instabilities of a falling film is investigated using the numerical technique of Li & Ji (1994). Previous analyses, such as the work by Whitaker (1964) and Lin (1970), are extended by taking into account the desorption of the surfactant.

The origin of our problem is found in a practice common in absorption refrigeration. Some surface-active agents, when added in small quantities, increase the capacity of absorption cooling machines (Bourne & Eisberg 1966). It is generally thought that the cause for this effect, occurring only in the presence of a surfactant, is Marangoni convection. That interfacial convection occurs and has this enhancing effect has been verified experimentally for pools of aqueous lithium bromide solutions absorbing water vapour (Kashiwagi, Kurosaki & Shishido 1985).

There are several analyses of Marangoni instabilities in mass or heat transfer systems (Pearson 1958; Scriven & Sternling 1964; Brian 1971; Brian & Ross 1972; Imaishi *et al.* 1983; McTaggart 1983; Castillo & Velarde 1985; Dijkstra 1988; Ho & Chang 1988; Goussis & Kelly 1990; Goussis & Kelly 1991; Pérez-Garcia & Carneiro 1991; Ji, Bjurström & Setterwall 1993). Brian (1971) and Brian & Ross (1972) showed that the surface excess of adsorbed solute opposes surface movement and delays or inhibits the

appearance of instability, even though the surface activity of solute is a prerequisite for instability: when it is desorbed, the surface tension of the liquid increases. Experimental verification of Brian's analysis was obtained by Imaishi *et al.* (1983).

However, previous studies of the Marangoni instabilities were mostly made on static films, or films with initially homogenous velocity. The mechanism of the improvement of the mass transfer rate by surface-active solute in falling films is not well understood. It is well known that isothermal flow down a vertical plane, in the absence of mass transfer processes such as evaporation or condensation, is unstable for all finite Reynolds numbers (Benjamin 1957; Yih 1963). Usually, an inactive surfactant has a stabilizing effect on falling films. Emmert & Pigford (1954) found experimentally that the addition of a wetting agent reduces rippling in falling liquid films. Whitaker (1964) indicated that surface elasticity was primarily responsible for the stabilizing action. Lin (1970) showed that both soluble and insoluble surfactants have a stabilizing effect on falling films, suppressing the natural wave instability. Several mechanisms may enhance or inhibit the instability of a falling film containing a surface-active solute and absorbing a vapour: adsorption of surfactant at the interface, its desorption from the liquid and the absorption process which includes both mass and heat transfer. Unstable modes other than those for an inert falling film may also appear.

The surface wave together with the thermocapillary instability have been studied for long-wavelength disturbances on a liquid film flowing down an inclined heated plane (Lin 1975; Kelly, Davies & Goussis 1986). The same problem but for disturbances of finite wavelength has been discussed in detail by Goussis & Kelly (1991). They indicated that three mechanisms cause the instabilities of the flow. One of them is associated with the shear stress of the basic flow at the deformed free surface and causes the instability of the surface wave. Both the other two mechanisms cause the thermocapillary instabilities. One is associated with the interaction of the basic temperature with the perturbation velocity field and causes thermocapillary instability of moderate-wavelength disturbances. The other one is associated with the modification of the basic temperature at the free surface by the surface deformation and causes thermocapillary instability of long-wavelength disturbances. The regions in their stability diagrams where each of the mechanisms dominates could be completely separated because they used a specific set of non-dimensional parameters in which the layer depth appears in one parameter only. Their results show that the instability can assume the form of either long transverse waves or short longitudinal rolls depending on which of the mechanisms that trigger the instabilities is dominant.

The mathematical model developed here includes desorption and Gibbs adsorption of surface-active agents. The effects of both phenomena on the instabilities of a falling liquid film are investigated. The critical conditions for instabilities and the fastest growing waves are determined. However, only instabilities in the form of transverse waves are studied in the present work.

2. Formulation of the problem

We consider a liquid film flowing down a vertical plane. Cartesian coordinates are used in writing the equations, with x^* in the direction of gravity, and y^* perpendicular to the plane. The origin of y^* is defined at the free surface of the primary flow, which

is assumed steady and parallel to the wall. Using the assumption of zero surface shear stress, the velocity profiled is obtained as

$$U^* = \frac{g}{2\nu}(d^2 - y^{*2}),$$

where U^* is the velocity, d the depth of the film, g the gravitational acceleration, and ν the kinematic viscosity. The velocity profile can also be written in dimensionless form:

$$U = 1 - y^2, \tag{1}$$

where $U = U^*/U_m$, U_m being the maximum velocity of the primary flow, equal to $gd^2/(2\nu)$, and $y = y^*/d$.

When analysing the stability of the primary flow, we may consider only two-dimensional disturbances (Yih 1963). In the model, all the physical properties will be assumed to be constants, except the surface tension. The basic equations for the problem are the equation of continuity:

$$\nabla \cdot \boldsymbol{u}^* = 0, \tag{2}$$

the incompressible Navier–Stokes equation:

$$\frac{\partial \boldsymbol{u}^*}{\partial t^*} + \boldsymbol{u}^* \cdot \nabla \boldsymbol{u}^* = -\frac{1}{\rho}\nabla p^* + \nu \nabla^2 \boldsymbol{u}^* + \boldsymbol{g}, \tag{3}$$

and the advection–diffusion equation for the surface-active solute:

$$\frac{\partial c_A^*}{\partial t^*} + \boldsymbol{u}^* \cdot \nabla c_A^* = D_A \nabla^2 c_A^*. \tag{4}$$

In the above equations, $\boldsymbol{u}^* = (u^*, v^*)$, where u^* and v^* denote the velocity components in the x^* and y^* directions respectively, t^* is the time, p^* the pressure, $\boldsymbol{g}$ the gravitational acceleration, ρ the density, ν the kinematic viscosity, c_A^* the bulk concentration of surface-active solute, and D_A the diffusivity of the surfactant in the solution.

At the free-surface boundary ($y^* = \eta^*$) the kinematic condition, the normal stress balance and the tangential stress balance can be formulated as follows:

$$\frac{\partial \eta^*}{\partial t^*} + u^* \frac{\partial \eta^*}{\partial x^*} = v^*, \tag{5}$$

$$p^* - p_g^* - 2\mu\left[\frac{\partial v^*}{\partial y^*} - \left(\frac{\partial v^*}{\partial x^*} + \frac{\partial u^*}{\partial y^*}\right)\frac{\partial \eta^*}{\partial x^*}\right] - \sigma \frac{\partial^2 \eta^*}{\partial x^{*2}} = 0, \tag{6}$$

$$2\mu\left(\frac{\partial v^*}{\partial y^*} - \frac{\partial u^*}{\partial x^*}\right)\frac{\partial \eta^*}{\partial x^*} + \mu\left(\frac{\partial v^*}{\partial x^*} + \frac{\partial u^*}{\partial y^*}\right) + \left(\frac{\partial \sigma}{\partial x^*} + \frac{\partial \eta^*}{\partial x^*}\frac{\partial \sigma}{\partial y^*}\right) = 0, \tag{7}$$

where η^* is the displacement of the free surface from its mean position, p_g^* the pressure in the gas phase, and σ the surface tension. When deriving these boundary equations, the surface deformation η^* has been assumed to be infinitesimal. The surface tension is here supposed to be a function of the concentration of surface-active solute, and a linear relationship is assumed:

$$\sigma = \sigma_0 + \left(\frac{\mathrm{d}\sigma}{\mathrm{d}c_A^*}\right)_0 (c_A^* - c_{A_0}), \tag{8}$$

where c_{A_0} is the initial concentration of the surface-active solute, and σ_0 the surface tension at c_{A_0}.

Two types of behaviour of the surface-active solute will be considered in the present

model: desorption from liquid phase to gas phase, and adsorption on the surface. However, the kinetics of adsorption are not considered in the present model We assume that the surface excess may be calculate by means of the Gibbs equation using the static surface tension. An experimental study by Yao, Bjurström & Setterwall (1991) on the surface tension of a lithium bromide aqueous solution in the presence of surfactants 1-octanol and 2-ethylhexanol suggests that the surface excess may be approximated by a constant in a certain range of concentrations below the solubility limit of the surfactant. In Brian's (1971) analysis of the effect of Gibbs adsorption on Marangoni instability, it was assumed that the 'Gibbs depth' is constant, which is reasonable for some surfactants in pure water. As mentioned in the Introduction, the goal of our work is to understand the effects of a surfactant in an absorption system, where a lithium bromide aqueous solution is usually used as working fluid. We adopt then the results for the surface tension from Yao *et al.* (1991) and assume in the model that the surface excess of surfactant is constant. The other two assumptions when deriving the boundary equation for the surface-active solute are that the concentration of the surface-active solute in the gas phase is zero and that there is equilibrium at the interface between the concentration in the gas phase and the concentration in the liquid phase. The mass balance for the surface-active solute at the interface, $y^* = \eta^*$, may be formulated as

$$D_A\left(\frac{\partial c_A^*}{\partial y^*}-\frac{\partial \eta^*}{\partial x^*}\frac{\partial c_A^*}{\partial x^*}\right)=\frac{k_G c_A^*}{m}+\Gamma^*\left(\frac{\partial u^*}{\partial x^*}+\frac{\partial \eta^*}{\partial x^*}\frac{\partial u^*}{\partial y^*}\right), \tag{9}$$

where k_G is the gas-phase mass transfer coefficient of the surface-active solute; m the solubility coefficient which is defined as the ratio of the concentration in liquid phase to the concentration in the gas phase at equilibrium, and Γ^* the surface excess concentration. In (9), the term on the left-hand side represents diffusion of the surfactant to the surface from the liquid beneath. The first term on the right-hand side represents the desorption, or evaporation, of the surfactant from the liquid phase into the gas phase. The second term multiplied by the surface excess concentration Γ^* represents mass transfer by advection of the surfactant within the adsorbed layer.

At the wall boundary, $y^* = d$, the no-slip velocity condition requires that

$$u^* = 0, \quad v^* = 0, \tag{10}$$

and the no-mass-flux condition requires that

$$\frac{\partial c_A^*}{\partial y^*} = 0. \tag{11}$$

Although the derivation of the linearized perturbation equations is trivial, we describe the main steps here for clarity. The governing equations are made dimensionless as follows:

$$(x,y)=\frac{(x^*,y^*)}{d}, \quad (u,v)=\frac{(u^*,v^*)}{U_m}, \quad t=\frac{t^*U_m}{d}, \quad p=\frac{p^*}{\rho U_m^2}, \quad c_A=\frac{c_A^*}{c_{A_0}}. \tag{12}$$

Each of the dimensionless variables, u, v, p and c_A, is then represented by the sum of the unperturbed value and an infinitesimal perturbation:

$$u = U+u', \quad v = v', \quad p = p_s+p', \quad c_A = c_{A_s}+c_A'. \tag{13}$$

The steady unperturbed concentration of the surface-active solution c_{A_s} is assumed

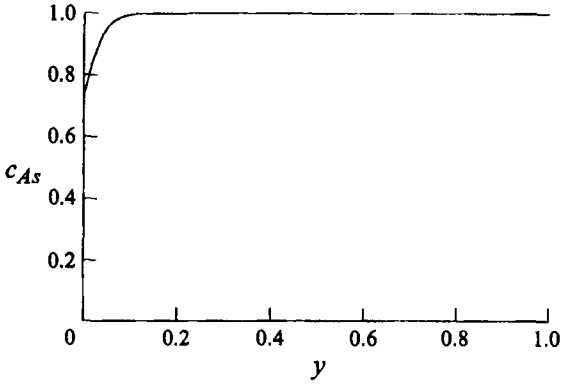

FIGURE 1. Basic-state concentration of surface-active solute ($Bi_A = 10, Pe_A = 10^6, x = 1000$).

to be a function of y only. It may be expressed in dimensionless form as follows, using the solution discussed in the Appendix:

$$c_{A_s}(y) = \operatorname{erf}(y_1) + \exp(g^2 - y_1^2)[1 - \operatorname{erf}(g)], \tag{14}$$

$$y_1 = \frac{y}{2(x/Pe_A)^{1/2}}, \quad g = y_1 + Bi_A (x/Pe_A)^{1/2},$$

with

$$Pe_A = \frac{U_m d}{D_A}, \quad Bi_A = \frac{k_G d}{m D_A}, \tag{15}$$

where x is dimensionless film length to be fixed in the calculations, Pe_A is the mass Péclet number for the additive, and Bi_A the Biot number. Figure 1 shows the profile of c_{A_s} calculated at $Bi_A = 10$, $Pe_A = 10^6$ and $x = 1000$ which corresponds to a 1 m length of the film if $d = 1$ mm.

Since the velocity perturbations satisfy the continuity equation, $\nabla \cdot \boldsymbol{u}' = 0$, a stream function ψ is introduced

$$u' = \psi_y, \quad v' = -\psi_x, \tag{16}$$

using subscripts to denote partial differentiation. Combining (12), (13) and (16) with the governing equations (2)–(7) and (9)–(11), using (1) and (8), and neglecting terms quadratic in the perturbation quantities, we obtain the following dimensionless perturbation equations:

$$\psi_{yt} + U\psi_{xy} - U_y \psi_x = -\frac{\partial p'}{\partial x} + \frac{1}{Re}\nabla^2 \psi_y, \tag{17}$$

$$-\psi_{xt} - U\psi_{xx} = -\frac{\partial p'}{\partial y} - \frac{1}{Re}\nabla^2 \psi_x, \tag{18}$$

$$\frac{\partial c'_A}{\partial t} + U\frac{\partial c'_A}{\partial x} - \psi_x \frac{\partial c_{A_s}}{\partial y} = \frac{1}{Pe_A}\nabla^2 c'_A, \tag{19}$$

with the boundary conditions at $y = 0$

$$\eta_t + \eta_x = -\psi_x, \tag{20}$$

$$p' + \frac{2}{Re}\psi_{xy} - \frac{1}{Re}\left[\frac{1}{Cr} + Ma_A(1 - c_{A_s})\right]\eta_{xx} = 0, \tag{21}$$

$$-\psi_{xx} + \psi_{yy} - 2\eta - Ma_A\left(\frac{\partial c'_A}{\partial x} + \eta_x \frac{\partial c_{A_s}}{\partial y}\right) = 0, \tag{22}$$

$$\frac{\partial c'_A}{\partial y} = Bi_A c'_A + \Gamma\psi_{xy} + \left(Bi_A \frac{\partial c_{A_s}}{\partial y} - \frac{\partial^2 c_{A_s}}{\partial y^2}\right)\eta, \tag{23}$$

and at $y = 1$

$$\psi_x = 0, \quad \psi_y = 0, \quad \frac{\partial c'_A}{\partial y} = 0. \tag{24}$$

In these equations Re is the Reynolds number, Cr is the Crispation number, Ma_A the Marangoni number, and Γ the adsorption number:

$$Re = \frac{U_m d}{\nu}, \quad Cr = \frac{\mu U_m}{\sigma_0}, \quad Ma_A = -\frac{(\partial\sigma/\partial c_A^*)_0 c_{A_0}}{\mu U_m}, \quad \Gamma = \frac{\Gamma^* U_m}{c_{A_0} D_A}. \tag{25}$$

The system is homogeneous in the x-direction because of the assumption that the unperturbed concentration c_{A_s} depends only on y. The perturbations may then be assumed to be of the normal mode form

$$\left.\begin{aligned} \psi &= \phi(y)\,e^{i\alpha(x-ct)}, \quad p' = P(y)\,e^{i\alpha(x-ct)}, \\ c'_A &= f(y)\,e^{i\alpha(x-ct)}, \quad \eta = \eta_0\,e^{i\alpha(x-ct)}, \end{aligned}\right\} \tag{26}$$

where α is the real wavenumber, and c is complex, $c = c_r + ic_i$. The wave velocity is c_r and the growth rate is given by αc_i.

Substituting (26) into the kinematic condition (20) yields

$$\eta_0 = -\phi(0)/(1-c). \tag{27}$$

Substituting (26) into (17)–(19), and eliminating P by cross-differentiation with the momentum equations, yields the well-known Orr–Sommerfeld equation

$$\frac{1}{i\alpha Re}\left(\frac{d^2}{dy^2} - \alpha^2\right)^2 \phi = (U-c)\left(\frac{d^2\phi}{dy^2} - \alpha^2\phi\right) - \frac{d^2U}{dy^2}\phi, \tag{28}$$

and the equation for the perturbed concentration of surfactant

$$\frac{1}{i\alpha Pe_A}\left(\frac{d^2 f}{dy^2} - \alpha^2 f\right) - (U-c)f = -\frac{\partial c_{A_s}}{\partial y}\phi. \tag{29}$$

Boundary conditions (20)–(24) become

$$-\phi'''(0) + [i\alpha Re(1-c) + 3\alpha^2]\phi'(0) + i\alpha^3\left[\frac{1}{Cr} + Ma_A(1-c_{A_s})\right]\frac{\phi(0)}{1-c} = 0, \tag{30}$$

$$-\phi''(0) + [-2 - \alpha^2(1-c) - i\alpha Ma_A c'_{A_s}(0)]\frac{\phi(0)}{1-c} + i\alpha Ma_A f(0) = 0, \tag{31}$$

$$-f'(0) + Bi_A f(0) + i\alpha\Gamma\phi'(0) - (Bi_A c'_{A_s}(0) - c''_{A_s}(0))\frac{\phi(0)}{1-c} = 0, \tag{32}$$

$$\phi(1) = 0, \quad \phi'(1) = 0, \quad f'(1) = 0, \tag{33}$$

in which the primes now denote differentiation with respect to y.

3. Solution procedure

3.1. *Integral boundary condition*

The simultaneous equations (28) and (29) together with their boundary conditions constitute an eigenvalue problem. This can be solved by using a numerical integration scheme in conjunction with a shooting method. But here we may treat (28) and (29)

separately since the function f couples to the fluid quantities only through the boundary conditions and does not appear in the internal Orr–Sommerfeld equation. We can then obtain an integral boundary condition which can be greatly simplified under certain circumstances. In this case, we need only to solve the single Orr–Sommerfeld equation. The numerical calculations of (28) with the integral boundary condition could be much faster than the direct calculations of the simultaneous equations (28) and (29).

To derive this integral boundary condition, we rewrite (29) as

$$\mathrm{L}f = -\mathrm{i}\alpha Pe_A\, c'_{A_s}\phi, \tag{34}$$

where the operator $\mathrm{L} = (\mathrm{d}^2/\mathrm{d}y^2) - \alpha^2 - \mathrm{i}\alpha Pe_A(U-c)$.

Let us consider the 'conjugate solution' of (34),

$$\mathrm{L}g = 0, \tag{35}$$

with the following boundary conditions:

$$g'(0) = -1, \quad g'(1) = 0. \tag{36}$$

The homogeneous equation (35) for g can be solved numerically using the efficient tridiagonal solver (Li & Ji 1994).

Now let us consider the relation

$$\int_0^1 (g\mathrm{L}f - f\mathrm{L}g)\,\mathrm{d}y = \int_0^1 (gf'' - fg'')\,\mathrm{d}y = -g(0)f'(0) + f(0)g'(0),$$

where the boundary conditions $f'(1) = 0$ in (33) and $g'(1) = 0$ in (36) have been used. On the other hand, from (34) and (35),

$$\int_0^1 (g\mathrm{L}f - f\mathrm{L}g)\,\mathrm{d}y = -\mathrm{i}\alpha Pe_A \int_0^1 g c'_{A_s}\phi\,\mathrm{d}y$$

so, we have

$$f(0)g'(0) - g(0)f'(0) = -\mathrm{i}\alpha Pe_A \int_0^1 g c'_{A_s}\phi\,\mathrm{d}y.$$

Combining this expression with (32), we obtain

$$f(0) = \frac{1}{g'(0) - g(0)\,Bi_A}\left\{g(0)\left[\mathrm{i}\alpha\Gamma\phi'(0) - (Bi_A\, c'_{A_s}(0) - c''_{A_s}(0))\frac{\phi(0)}{1-c}\right] - \mathrm{i}\alpha Pe_A \int_0^1 g c'_{A_s}\phi\,\mathrm{d}y\right\}. \tag{37}$$

The integral boundary condition is then obtained by inserting (37) into (31) as follows:

$$\phi''(0) + \alpha^2\phi(0) - U''\frac{\phi(0)}{1-c} + \frac{\mathrm{i}\alpha Ma_A}{g'(0) - g(0)\,Bi_A} \times \left[(g'(0)\,c'_{A_s}(0) - g(0)\,c''_{A_s}(0))\frac{\phi(0)}{1-c} - g(0)\,\mathrm{i}\alpha\Gamma\phi'(0) + \mathrm{i}\alpha Pe_A \int_0^1 g c'_{A_s}\phi\,\mathrm{d}y\right] = 0. \tag{38}$$

This equation contains an integral with respect to ϕ, which can be interpreted as a global 'boundary' condition involving all values of ϕ along the y-coordinates. However, the function c'_{A_s} is almost zero everywhere except in the vicinity of the interface, see figure 1. This enables us to expand ϕ and therefore to express the integral as a Taylor expansion. In general, we write

$$\int_0^1 g c'_{A_s}\phi\,\mathrm{d}y = \sum_{k=0}^{\infty} \frac{\phi^{(k)}(0)}{k!} \int_0^1 g c'_{A_s} y^k\,\mathrm{d}y = \sum_{k=0}^{\infty} \phi^{(k)}(0)\, M_k, \tag{39}$$

in which M_k is defined as

$$M_k = \frac{1}{k!}\int_0^1 gc'_{A_s} y^k \, dy.$$

The magnitude of M_k is expected to decay rapidly and it has been verified in the calculations that the first four or five terms in the expansion (39) are enough to keep the accuracy. Taking the first four terms, we may write

$$\int_0^1 gc'_{A_s}\phi \, dy = \phi(0)M_0 + \phi'(0)M_1 + (\psi(0)+\alpha^2\phi(0))M_2 + (\psi'(0)+\alpha^2\phi'(0))M_3, \quad (40)$$

and by introducing the function ψ,

$$\psi = \phi'' - \alpha^2\phi, \quad (41)$$

we can write the Orr–Sommerfeld equation as a set of second-order equations (Li & Ji 1994).

3.2. *Numerical scheme*

The numerical technique developed by Li & Ji (1994) for solving the Orr–Sommerfeld equation in the case of a single-component falling film flow is employed here for the solution of the extended eigenvalue problem when a surfactant is present. The main feature of the scheme is that the discretized matrix has a block-tridiagonal form. Compared to a straightforward finite-difference scheme in conjunction with a shooting method, it may have the following advantages. (i) It is faster. The calculation for a tridiagonal matrix by Guassian elimination is proportional to n, where n denotes the number of grid points. But the calculation using a finite-difference method is proportional to n^3. (ii) The scheme is very simple to implement.

Compared with the equations for a pure falling film flow without any heat or mass transfer (Li & Ji 1994), there are changes neither in the inner (Orr–Sommerfeld) equation, (28), nor in the wall boundary conditions, (33). The differences arise in the two boundary conditions at the interface: the presence of a surfactant in the film requires a modification of the normal force balance and of the tangential force balance. These will degenerate to the equations for pure falling film flows when $Ma_A = 0$. The numerical scheme for solving this eigenvalue problem has been described in detail in Li & Ji (1994). The scheme uses a Taylor expansion to discretize the differential eigen-equation into an algebraic one with block tridiagonal form. This system can be solved by Gaussian elimination. The equation matrix may be written as

$$\boldsymbol{D} = \begin{pmatrix} \boldsymbol{a}_{11} & \boldsymbol{a}_{12} & \cdots & \boldsymbol{a}_{i;m+1} & & \\ \boldsymbol{A}_2 & \boldsymbol{B}_2 & \boldsymbol{C}_2 & & & \\ \cdots & & & & & \\ & & & \boldsymbol{A}_{n-1} & \boldsymbol{B}_{n-1} & \boldsymbol{C}_{n-1} \\ & & \boldsymbol{a}_{n;n-m} & \cdots & \boldsymbol{a}_{n;n-1} & \boldsymbol{a}_{nn} \end{pmatrix}, \quad (42)$$

in which the block matrices are all 2×2. Formulae for the inner points $\boldsymbol{A}_i, \boldsymbol{B}_i, \boldsymbol{C}_i, i = 2, n-1$, are given by Li & Ji (1994) for a sixth-order Taylor expansion, together with the formulae for the wall boundary $\boldsymbol{a}_{nk}, k = n-m, n$. Here, we state only the part of the matrix that differs from that of Li & Ji (1994): the block matrix $\boldsymbol{a}_{1k}, k = 1, m+1$, in the first line.

Using (40) and (41), the two boundary equations (30) and (38) at the interface may then be written in the form:

$$a_1\psi(0) + a_2\psi'(0) + b_1\phi(0) + b_2\phi'(0) = 0, \quad (43)$$

$$c_1\psi(0) + c_2\psi'(0) + d_1\phi(0) + d_2\phi'(0) = 0, \quad (44)$$

where

$$a_1 = 0, \quad a_2 = -1,$$

$$b_1 = \left[\frac{1}{Cr} + Ma_A(1-c_{A_s}(0))\right]\frac{\mathrm{i}\alpha^3}{1-c}, \quad b_2 = \mathrm{i}\alpha Re(1-c)+2\alpha^2,$$

$$c_1 = 1+\beta_4\,\mathrm{i}\alpha Pe_A M_2, \quad c_2 = \beta_4\,\mathrm{i}\alpha Pe_A M_3$$

$$d_1 = 2\alpha^2 - \frac{U''}{1-c} + \beta_4\left[\frac{g'(0)c'_{A_s}(0)-g(0)c''_{A_s}(0)}{1-c} + \mathrm{i}\alpha Pe_A(M_0+\alpha^2 M_2)\right],$$

$$d_2 = \beta_4[-g(0)\,\mathrm{i}\alpha\Gamma + \mathrm{i}\alpha Pe_A(M_1+\alpha^2 M_3)], \quad \beta_4 = \frac{\mathrm{i}\alpha Ma_A}{g'(0)-g(0)\,Bi_A}.$$

We may write the derivatives $\phi'(0)$ and $\psi'(0)$ to mth-order accuracy as

$$\phi'(0) = \frac{1}{h}\sum_{k=1}^{m+1}\mu_k\phi_k, \quad \psi'(0) = \frac{1}{h}\sum_{k=1}^{m+1}\mu_k\psi_k.$$

Here, h is the spacing of the grid mesh. The coefficients μ_k can be derived from the approximate expression for the functions from the mth-order Lagrange polynomial, as shown in Li & Ji (1994) for $m = 2, 4, 8$. The block matrices on the first line of the equation matrix are then

$$\boldsymbol{a}_{11} = \begin{pmatrix} ha_1+a_2\mu_1 & hb_1+b_2\mu_1 \\ hc_1+c_2\mu_1 & hd_1+d_2\mu_1 \end{pmatrix},$$

$$\boldsymbol{a}_{1k} = \begin{pmatrix} a_2\mu_k & b_2\mu_k \\ c_2\mu_k & d_2\mu_k \end{pmatrix}, \quad k = 2, 3, \ldots, m+1.$$

4. Results and discussion

In all the cases discussed below, the Crispation number Cr is chosen as 0.2, and the mass Péclet number Pe_A is chosen as 10^6.

4.1. *Spectrum; new eigenmode*

Spectra of the eigen-equation for falling liquid films without surfactant have already been investigated in detail (Li & Ji 1994). Two modes were found to become unstable for certain Reynolds numbers or wavenumbers: the so-called surface wave and 'wall wave'. The structure of the spectra for $Re = 20$ and $\alpha = 1$ is shown in figure 2(*a*) for falling films without surfactant, and in figure 2(*b*) for falling films with a surfactant but with $Ma_A = 0$. It is seen by comparing the two figures that there is an additional mode in figure 2(*b*). This new mode may be explained as follows: when deriving the integral boundary equation (38) it was noted that the perturbed concentration f couples to the fluid equations only through the boundary conditions. Furthermore, the advection–diffusion equation decouples to the fluid equations when $Ma_A = 0$, see (30) and (31). Therefore, in the case $Ma_A = 0$ of figure 2(*b*), one may interpret the new mode as that for which the disturbed velocity ϕ is trivial, but the disturbed concentration f has an independent non-trivial solution.

Actually, there is not just only one new mode from the advection–diffusion equation of surfactant. This cannot be shown completely in the plot of figure 2(*b*) because of the difference of scale between the modes and some numerical limitations. A plot of the spectrum for the eigen-equation of the transport of surfactant with the same parameter values as figure 2(*b*) is given in figure 3(*a*). One can see that the real part of the spectrum of the new modes is close to 1, especially for the first ones. This means that

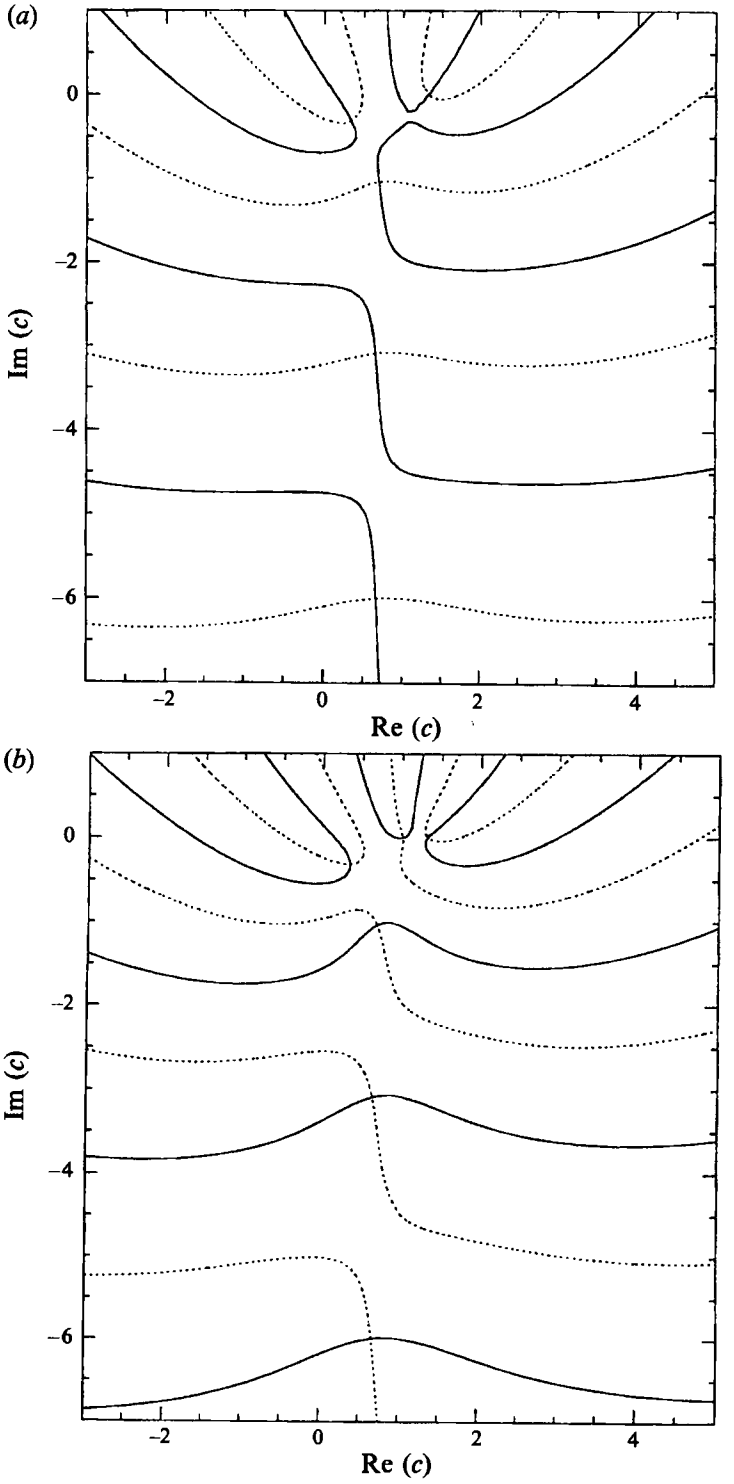

FIGURE 2. Spectra in the c-plane for the falling film (a) without surfactant and (b) with surfactant ($Bi_A = 10, Ma_A = 0$), at $Re = 20, \alpha = 1$. Intersections between solid and dotted curves are points of the spectrum. The solid lines are zero contours of the real part of $D(c)$, and the dotted lines are zero contours of the imaginary part.

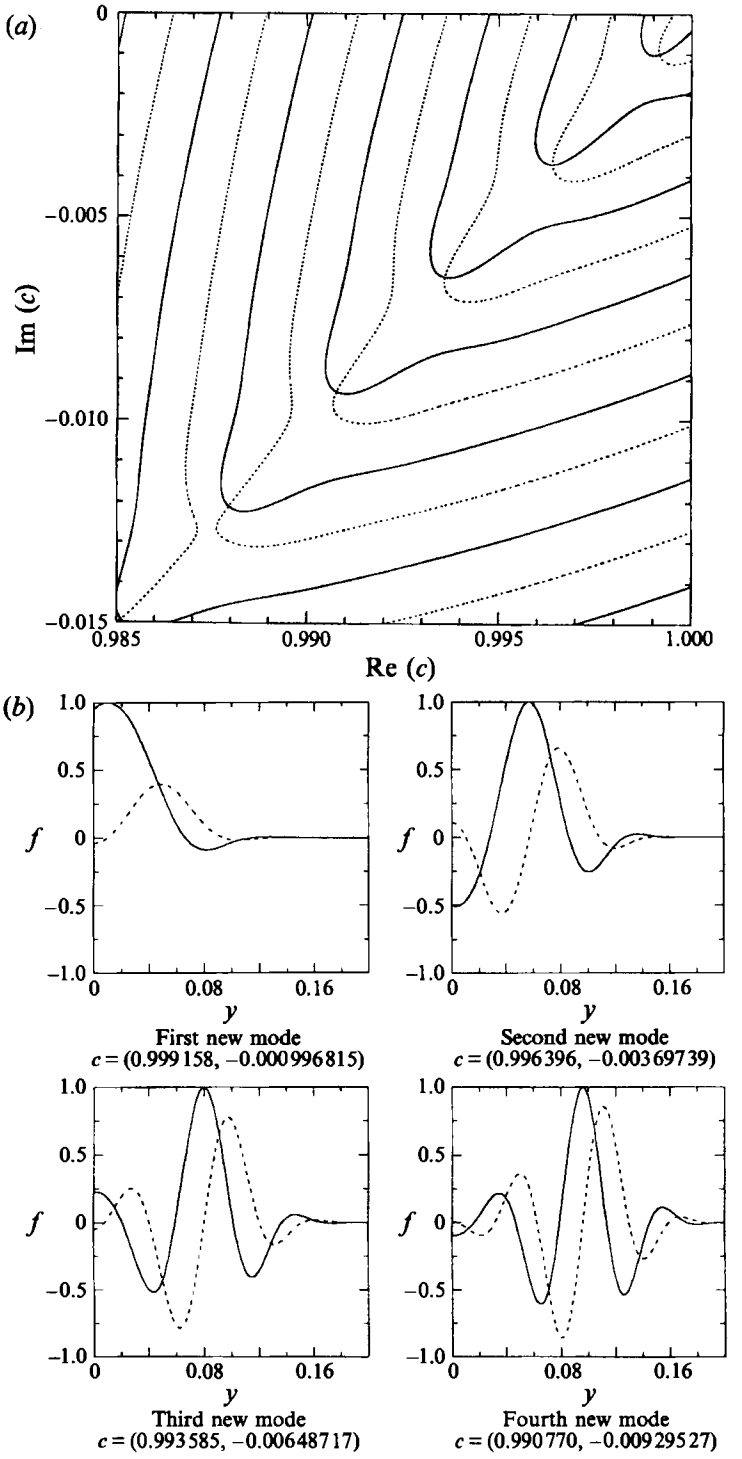

FIGURE 3(*a*) Spectrum in the c-plane for the eigen-equation of the advection–diffusion equation of surface-active solute with zero perturbed velocity ((29) with $\phi = 0$) ($\alpha = 1$, $Bi_A = 10$ and $Pe_A = 10^6$). (*b*) Eigenfunctions of the first 4 modes for the advection–diffusion of surfactant ($\alpha = 1$ and $Bi_A = 10$). The solid lines represent the real part of the eigenfunctions, and the dashed lines the imaginary part. The eigenvalue for each mode is shown under its graph.

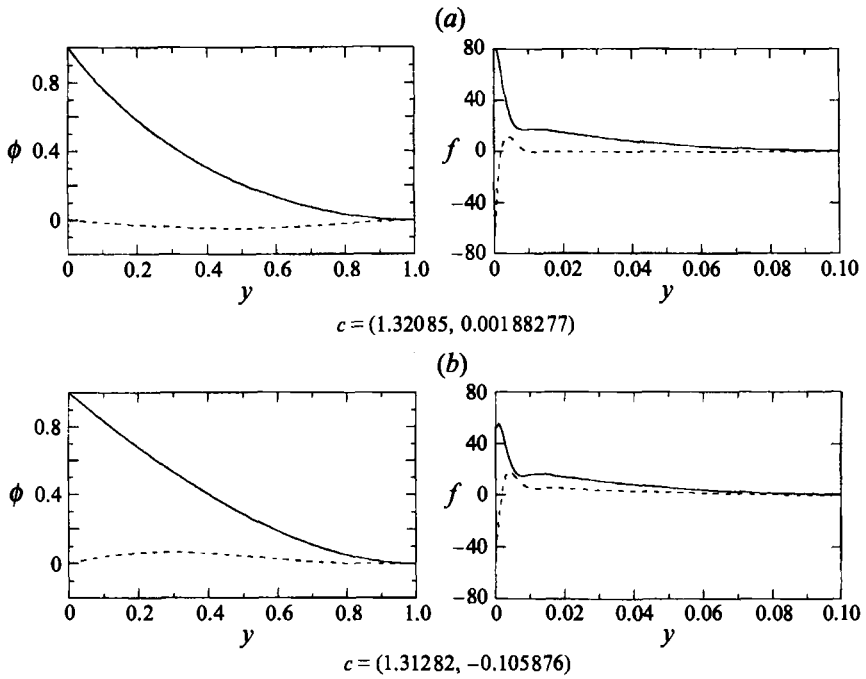

FIGURE 4. Eigenfunctions of the surface wave with Marangoni number as parameter ($Re = 20$, $\alpha = 1$ and $Bi_A = 10$). The solid lines represent the real part of the eigenfunctions, and the dashed lines the imaginary part. The eigenvalue for each case is shown under its graph. (*a*) $Ma_A = 0$, (*b*) $Ma_A = 1$.

Ma_A	$Re = 5000$	$Re = 10000$
0	$c = (0.267840, -1.75271\text{D-}03)$	$c = (0.237413, 3.75806\text{D-}03)$
2	$c = (0.267807, -1.75310\text{D-}03)$	$c = (0.237400, 3.76006\text{D-}03)$
4	$c = (0.267775, -1.75352\text{D-}03)$	$c = (0.237388, 3.76206\text{D-}03)$
6	$c = (0.267742, -1.75398\text{D-}03)$	$c = (0.237375, 3.76406\text{D-}03)$
8	$c = (0.267710, -1.75448\text{D-}03)$	$c = (0.237362, 3.76604\text{D-}03)$
10	$c = (0.267677, -1.75500\text{D-}03)$	$c = (0.237350, 3.76802\text{D-}03)$

TABLE 1. Eigenvalues of the 'wall wave' mode of the falling film ($\alpha = 1, Bi_A = 10, \Gamma = 2000$)

the wave velocity of the modes is close to the surface velocity of the falling film. The eigenfunctions of the perturbed concentration of surfactant are shown in figure 3(*b*) for the first four modes, numbering the modes here according to the values of their imaginary parts. The eigenvalue for each mode is given below the corresponding plot of the function. It can be clearly seen that modes of higher mode number have a more oscillatory structure and are more stable. It has been verified in the calculations that the eigenfunction f is equivalent to the function g for the special case $Ma_A = 0$. Its eigenvalues depend only on α, Bi_A and Pe_A and satisfy the following equation:

$$g'(0) - g(0)\, Bi_A = 0.$$

Since these new modes exist even if the velocity field is unperturbed, when $Ma_A = 0$, they are the solution of the eigen-equation derived from the advection–diffusion equation for the surfactant with the primary parabolic velocity. They may be called 'diffusion waves'. The eigenvalues in figure 3(*b*) show that these waves are

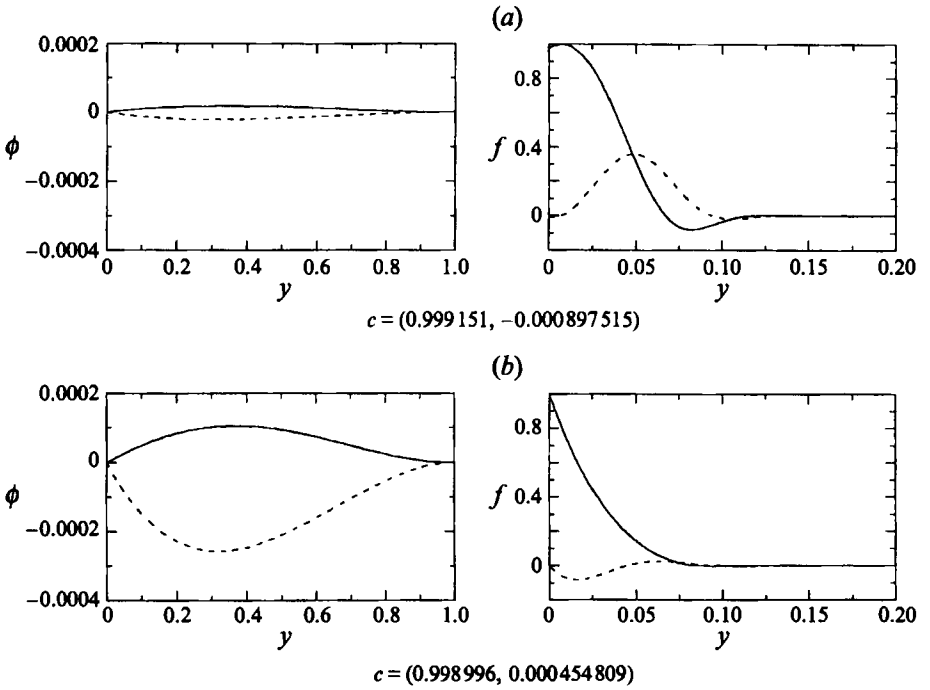

FIGURE 5. Eigenfunctions of the 'diffusion wave' with Marangoni number as parameter ($Re = 20$, $\alpha = 1$ and $Bi_A = 10$). The solid lines represent the real part of the eigenfunctions, and the dashed lines the imaginary part. The eigenvalue for each case is shown under its graph. (*a*) $Ma_A = 0.01$, (*b*) $Ma_A = 1$.

decaying, as the imaginary parts of the growth rate ω, defined as $\omega = \alpha c$, are negative. When the advection–diffusion equation and the fluid equations are coupled with each other through the boundary conditions at the interface, i.e. when $Ma_A \neq 0$, 'diffusion waves' develop, and one finds that only the first mode may become unstable. We shall, then, discuss this first mode in more detail but not the other new modes, and we call it a 'diffusion wave' in the following to distinguish it from the waves associated with a falling film flow without surfactant.

4.2. *Effect of Ma_A on the unstable modes*

Figure 4 shows the dependence of the eigenfunctions of the surface wave on the Marangoni number. The parameters in the calculations have the following values: $Re = 20$, $\alpha = 1$, $Bi_A = 10$ and $\Gamma = 2000$. The solid lines represent the real part of the eigenfunctions, and the dashed lines represent the imaginary part. The functions are scaled using the maximum value of ϕ. The eigenvalue for each case is shown under the graphs. It can be seen that as Ma_A increases, the ratio of function f to function ϕ becomes smaller, and the mode becomes more stable.

The calculations show that Ma_A has only a limited effect on the 'wall wave' mode of falling films, see table 1. This is what we expect since the 'wall wave' mode is mainly associated with the wall, as its name indicates. The Marangoni number is introduced in the boundary equations of the interface, and thus its effect is largely near the interface. This 'wall wave' mode will be discussed no further since we are more interested in the instabilities of falling films at low or moderate Reynolds numbers.

Figure 5 shows the eigenfunctions with the same parameter values as in figure 4 but for the new 'diffusion wave'. Here, we use the maximum value of f to scale the two

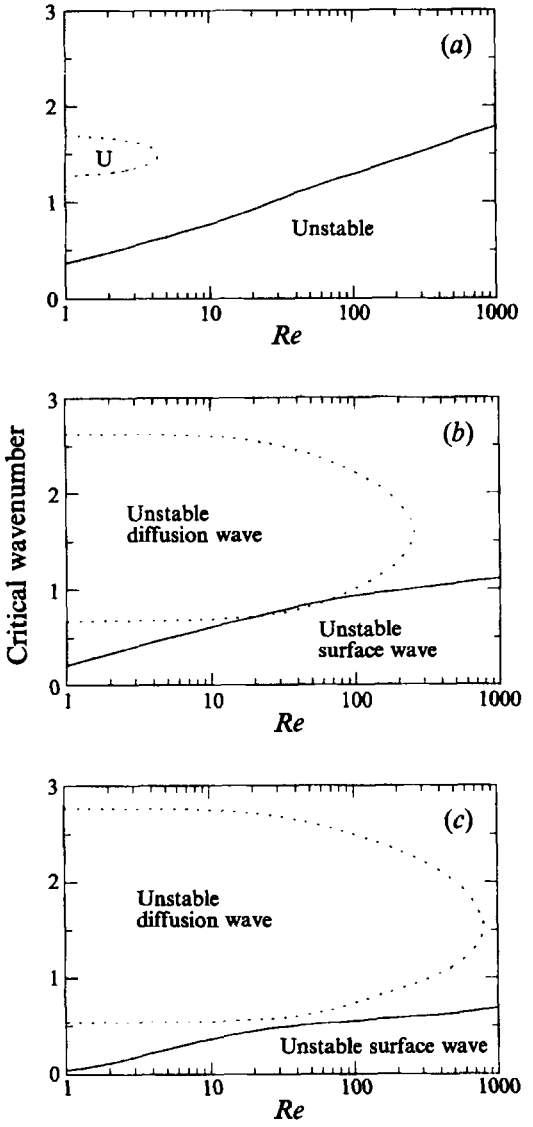

FIGURE 6. Neutral curve of the surface wave (——) and the 'diffusion wave' (-----) in the (α, Re)-plane with Marangoni number as parameter ($Bi_A = 10, \Gamma = 2000$). (*a*) $Ma_A = 0.15$, (*b*) $Ma_A = 0.6$, (*c*) $Ma_A = 2$.

functions instead of ϕ as in figure 4 because ϕ tends to zero as Ma_A tends to zero for this mode. It is seen that the ratio of ϕ to f is much smaller than that of the surface wave, but it becomes larger as Ma_A increases, similarly to figure 4. The results for eigenvalue c show that the mode may become unstable for large Ma_A, which is in contrast to the results for the surface wave. The reason for the mode becoming unstable may be the Marangoni effect. When $Ma_A \neq 0$, the concentration f couples to the velocity ϕ through the tangential force balance at the interface. The surface tension gradient caused by the surfactant concentration gradient may induce Marangoni convection.

The domains of instabilities for both the surface wave and the 'diffusion wave'

modes are illustrated in figure 6(*a–c*) using the neutral curves in the (α, *Re*)-plane to show their boundaries. The parameter values are $\Gamma = 2000$, $Bi_A = 10$ and $Ma_A = 0.15$, 0.6 *and* 2. Marangoni convection corresponding to the 'diffusion wave' occurs at larger wavenumbers than that of the surface wave mode. The larger Ma_A is, the smaller is the unstable region for the surface wave and the larger is the unstable region for the 'diffusion wave'.

The growth rate of the perturbations, defined by αc_i with c_i the imaginary part of c, is illustrated in figure 7 as contour plots in the (α, *Re*)-plane for both the surface wave (figure 7*a*) and the 'diffusion wave' (figure 7*b*). The domains of instabilities are those where the growth rate is positive. The 'diffusion wave' seems to be much weaker than the surface wave: the maximum growth rate is much smaller than that of the surface wave. This is not necessarily always so for all values of the parameters. As Ma_A increases, for example, the growth rate of the diffusion wave increases and the growth rate of the surface wave decreases; the two waves may become comparable with each other. Figure 7(*b*) indicates that the most unstable wave of the 'diffusion wave' occurs at small Reynolds numbers.

Let us now investigate more closely the marginal state, for which the imaginary part of the phase velocity c is zero, and the most unstable waves for the model system. The parameters related to the presence of a surfactant are the Biot number Bi_A, the adsorption number Γ and the Marangoni number Ma_A.

4.3. *Effects of surface-active solute on the surface wave*

From the plots of the neutral curves in figure 6, one sees that, as Ma_A increases, the critical wavenumber of the surface wave decreases: in other words, the unstable region in the (α, *Re*)-plane becomes smaller. This increased stability is also found in plots of the dependence of the most unstable wave on Ma_A in figure 8. The conclusion is that, as is well-known, the presence of a surfactant restrains the surface wave. As Ma_A increases, the wavenumber of the most unstable wave decreases as does its growth rate. But the wave velocity for the most unstable wave increases as Ma_A increases.

The effect of Bi_A and Γ on the mode is illustrated in figure 9(*a–d*). Adsorption of surfactant has a stabilizing effect on the surface wave. A higher Γ results in smaller wavenumbers both for the neutral wave and the most unstable wave, and in a lower growth rate for the most unstable wave. But the wave velocity of the most unstable wave increases as Γ increases. Varying Bi_A in a wide range, from 1 to 100, shows that desorption of surfactant has only a small effect on the surface wave in comparison with that of Γ or Ma_A. The effect of Bi_A may be larger for a higher Γ and a higher Bi_A itself. In such a case, the effect of Bi_A on the critical wavenumbers and the parameters of the most unstable wave is opposite to that of Γ, see figure 9.

In the previous analyses (Whitaker 1964; Whitaker & Jones 1966; Lin 1970) for the flow of a film covered with soluble or insoluble surface-active agents, it was found that both soluble and insoluble surface-active agents have stabilizing effects. (Lin 1970 pointed out that his analysis is only for the instability due to the long surface wave.) Since the desorption of the surface-active agent was not considered in their model, the Marangoni instability is thus not likely to occur. Here, we consider only soluble surface-active agents, but the boundary condition is more complex, including the desorption of the surfactant. Figure 9 indicates that the stabilizing effect of a surface-active agent on the surface wave depends strongly on the adsorption number Γ. This is in accordance with the results of previous authors. The accumulation of the surface-active substances at the surface could stabilize the film flow through its effect on the tangential surface tension force, as explained by Lin (1970).

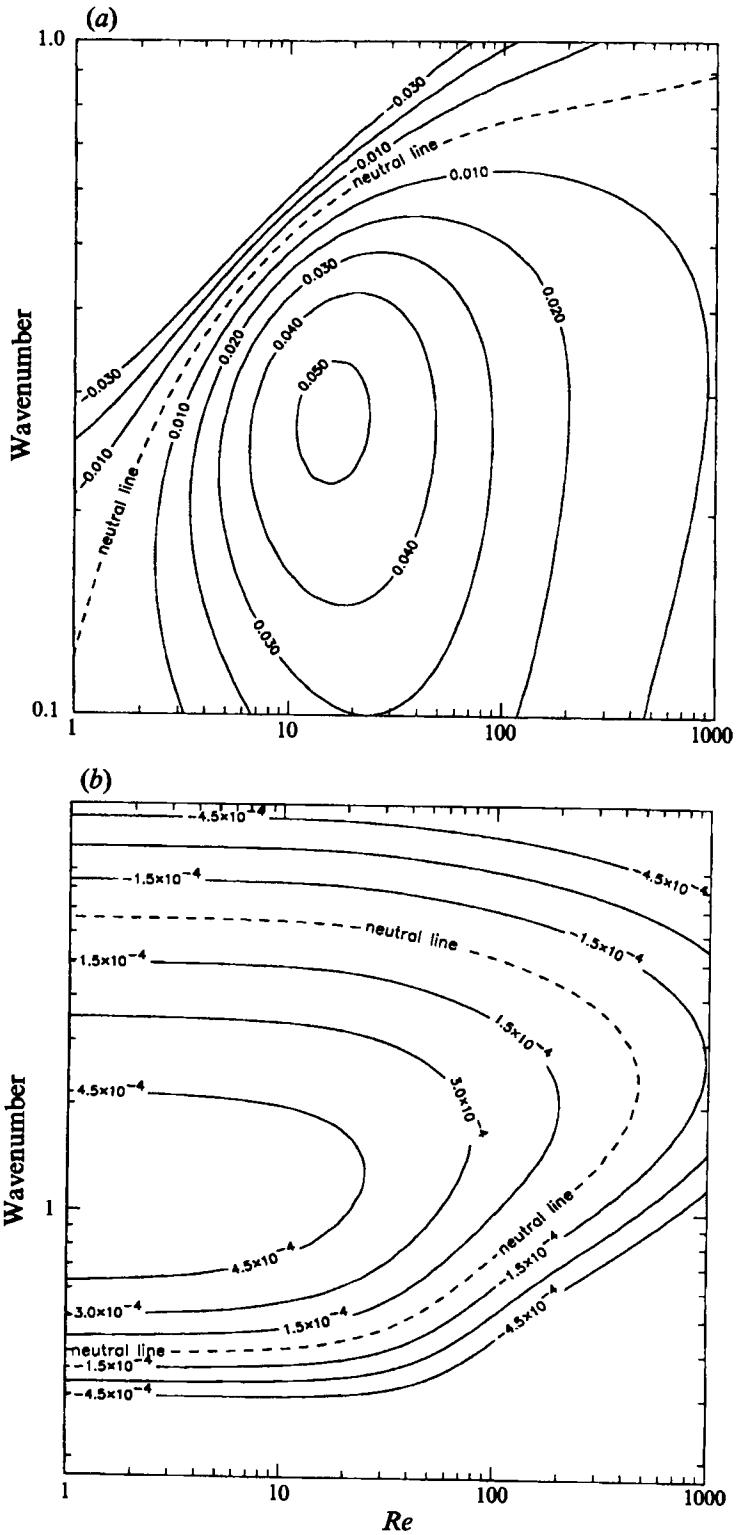

FIGURE 7. Contour plot for the growth rates of disturbances in (α, Re)-plane for (*a*) the surface wave and (*b*) the 'diffusion wave' ($Bi_A = 10$, $Ma_A = 1$ and $\Gamma = 2000$).

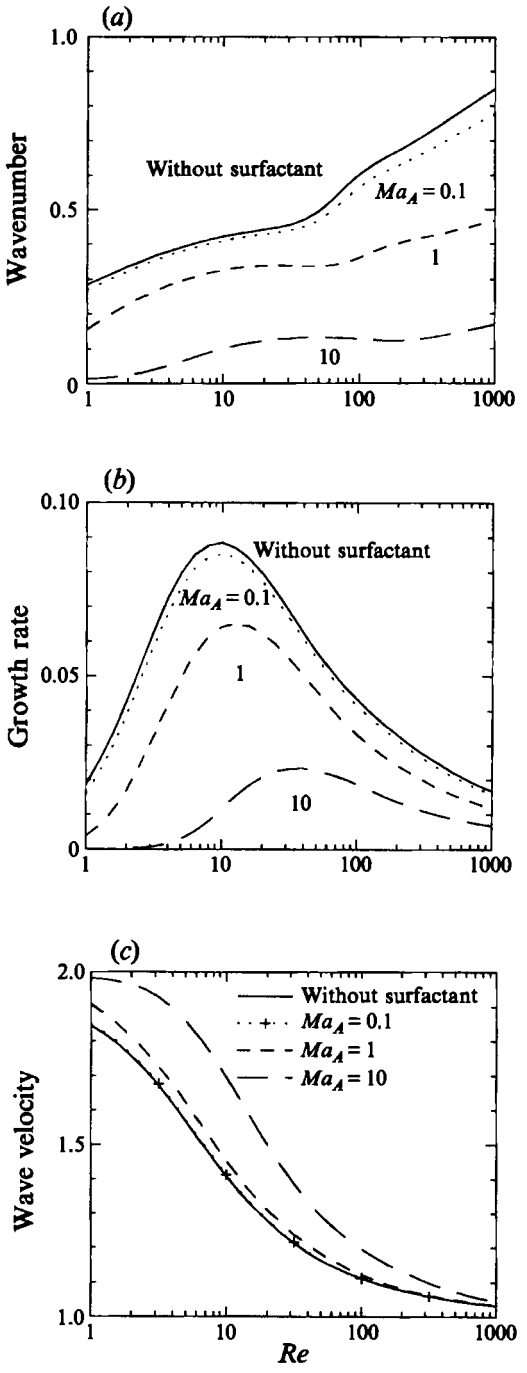

FIGURE 8(*a–c*). Dependence of the most unstable wave of the surface wave on the Marangoni number at $Bi_A = 10$ and $\Gamma = 2000$.

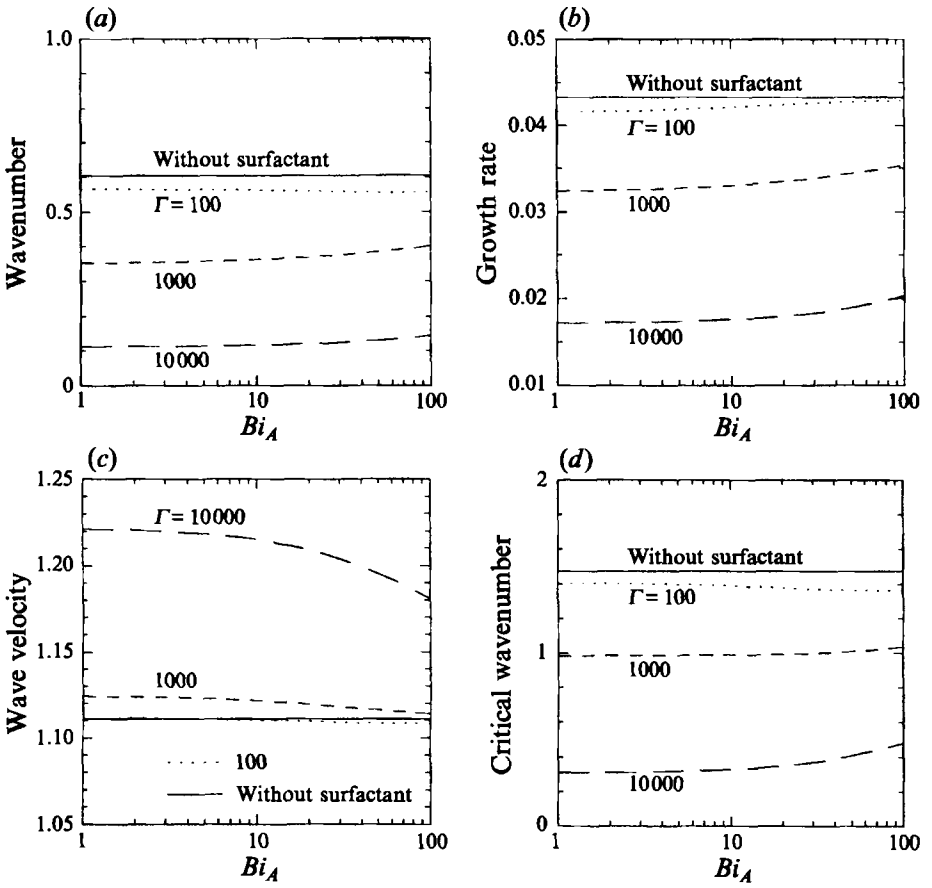

FIGURE 9(*a–d*). Effects of Biot number and adsorption number on the most unstable wave and the neutral wave of the surface wave at $Ma_A = 1, Re = 100$.

4.4. *Effects of surface-active solute on the 'diffusion wave'*

The plots in figure 6 show that the unstable region of the mode of a 'diffusion wave' in the (α, Re)-plane is larger for a larger Ma_A. Figure 10(*a–c*) shows the effect of Ma_A on the most unstable waves of the mode. The wavenumber having maximum growth rate decreases as Ma_A increases. The maximum growth rate increases as Ma_A increases.

The effect of the Biot number Bi_A on the critical waves and the most unstable waves of the mode is illustrated in figure 11 (*a–d*). In the calculations, $Ma_A = 1$ and $\Gamma = 2000$. The unstable region in the (α, Re)-plane becomes larger as Bi_A increases, see figure 11(*a*). For the most unstable waves, the wavenumber increases, wave velocity increases, and the growth rate increases as Bi_A increase. These results indicate that a faster evaporation rate of surfactant from liquid phase to gas phase causes the mode to be more unstable.

Contrary to the destabilizing effect of the desorption of surfactant, the adsorption of surface-active solute tends to inhibits the Marangoni convection. As shown in figure 12(*a–d*), the unstable region in the (α, Re)-plane becomes smaller as Γ increases, and it may disappear when Γ exceeds a certain value. For the most unstable waves, the wavenumber, the wave velocity and the growth rate all decrease as Γ increases.

A better understanding of this mode is obtained by examination of figure 13, a plot

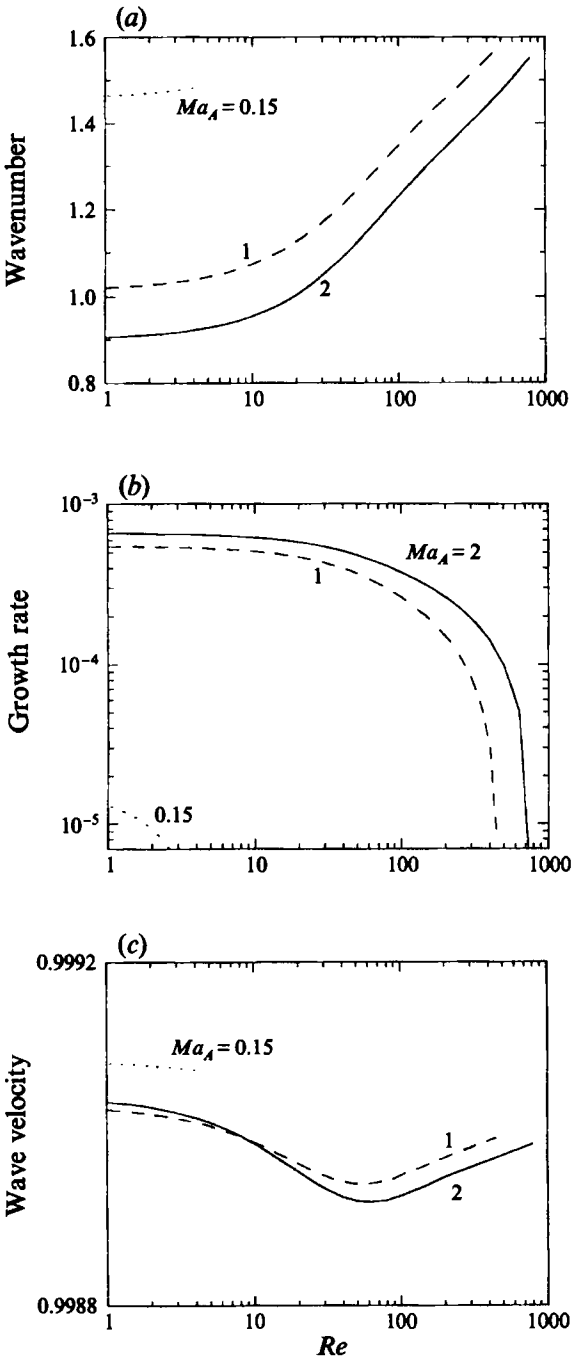

FIGURE 10(*a–c*). Dependence of the most unstable wave of the 'diffusion wave' on the Marangoni number at $Bi_A = 10$ and $\Gamma = 2000$.

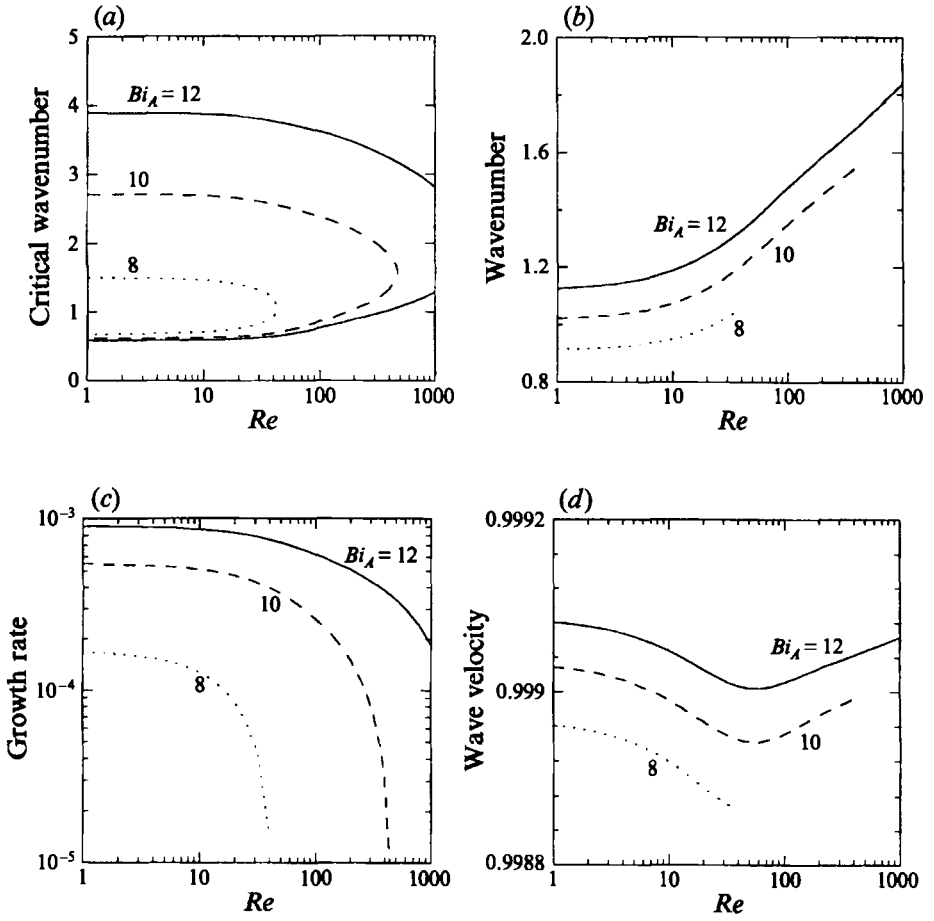

FIGURE 11(*a–d*). Effect of Biot number on the critical wave and the most unstable wave of the 'diffusion wave' at $Ma_A = 1$ and $\Gamma = 2000$.

of neutral curves for the 'diffusion wave' in the (Ma_A, α)-plane. For a fixed Reynolds number there is a critical Marangoni number, defined here as the minimum in the neutral curve in the (Ma_A, α)-plane and denoted by Ma_{Ac}, below which there is no Marangoni instability of the 'diffusion wave'. The figure shows that conditions for Marangoni convection are more favourable when the Reynolds number is smaller. The dependence of Ma_{Ac} on Bi_A and Γ is shown for $Re = 50$ in figure 14(*a*) and figure 14(*b*) respectively. Ma_{Ac} increases when Γ increases or Bi_A decreases. It tends towards infinity when Bi_A becomes very small or when Γ tends to a certain high value, in which cases the 'diffusion wave' will never become unstable. The results demonstrate that desorption of the surfactant (Bi_A) is necessary to produce the Marangoni instability, while adsorption of the surfactant (Γ) could completely suppress the instability.

Goussis & Kelly (1990) in their studies of a horizontal liquid layer heated from below indicated that there are two distinct mechanisms by which thermocapillary instabilities may be triggered. One mechanism is associated with the interaction of the basic temperature with the perturbation velocity field. This type of instability was first examined by Pearson (1958) who assumed a rigid free surface. The 'diffusion wave'

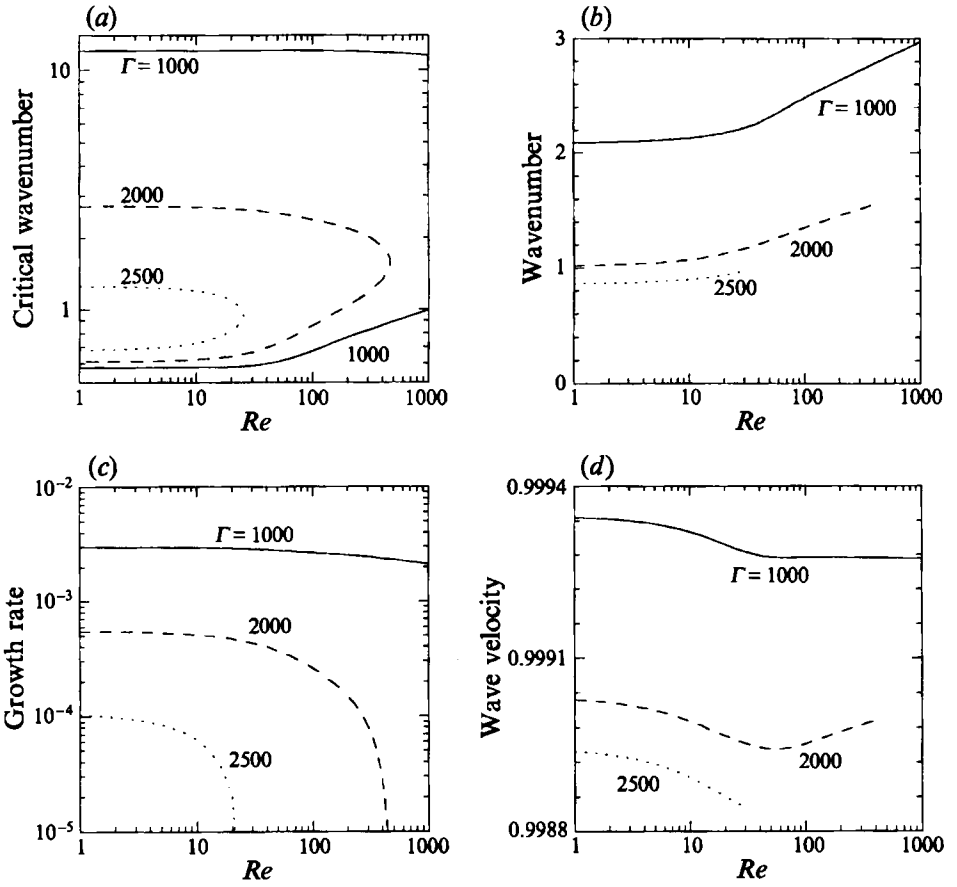

FIGURE 12(*a–d*). Effect of adsorption number on the critical wave and the most unstable wave of the 'diffusion wave' at $Ma_A = 1$ and $Bi_A = 10$.

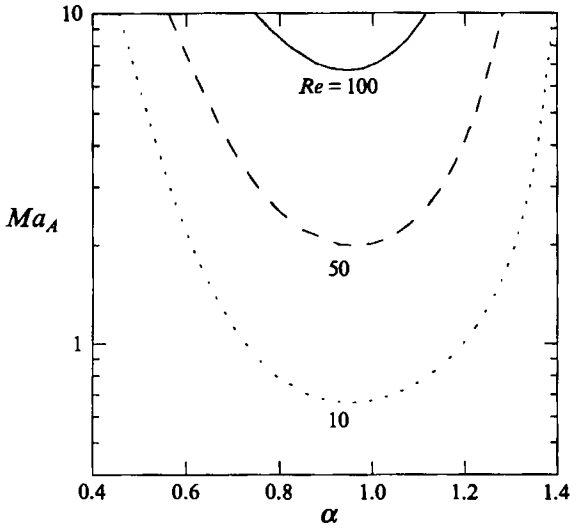

FIGURE 13. Neutral curves of the 'diffusion wave' in the (α, Ma_A) plane with Reynolds number as parameter ($Bi_A = 10, \Gamma = 2500$).

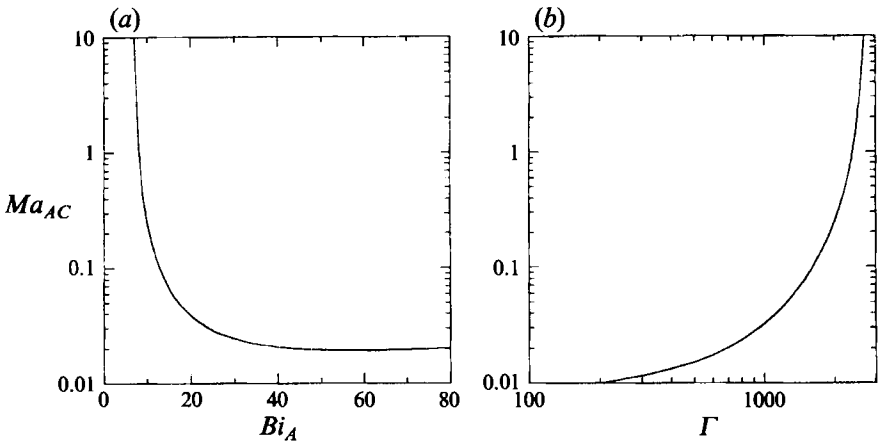

FIGURE 14. Dependence of the critical Marangoni number on (*a*) the Biot number at $\Gamma = 2000$, and (*b*) the adsorption number at $Bi_A = 10$, ($Re = 50$).

reported here may be interpreted as a Marangoni instability of this type by comparing figure 13 with the stability diagrams reported by Pearson. The other mechanism is associated with the modification of the basic temperature at the free surface by the surface deformation and causes thermocapillary instability of large-wavelength disturbances. This type of instability in the present model will be discussed in next subsection.

We note that in the stability diagrams reported by Pearson (1958) the thermocapillary instability is more stable for a larger heat transfer at the interface, the transfer rate being represented by parameter L in his article. But our results here show that the 'diffusion wave' is more unstable for a higher evaporation rate of the surfactant (Bi_A). This may be explained as follows. In our model the basic concentration, which is given by (14), depends on the parameter Bi_A, but in Pearson's model the basic temperature is predefined and is independent of the parameter L. It has been verified in the calculations that if the basic concentration is fixed, an increase in Bi_A will lead to a more stable 'diffusion wave'. Since the mechanism for the instability of a 'diffusion wave' is associated with the interaction of the basic concentration with the perturbation velocity field, according to the analyses given by Goussis & Kelly (1990), a higher Bi_A in the basic state will result in a steeper basic concentration and thus a more unstable 'diffusion wave'. On the other hand, a higher Bi_A for the perturbed concentration will reduce the surface tension driving force for the instability. Clearly the destabilizing effect of desorption of the surfactant on the 'diffusion wave' shown in figure 11 is because of its effect in producing a non-uniform basic concentration.

4.5. *Marangoni instability of long-wave disturbances*

We shall examine the Marangoni instability of long wave disturbances in this subsection to complete the study.

Goussis & Kelly (1991) concluded for a thin film flowing down a heated plate that three mechanisms exist to cause the instabilities of the flow. One mechanism is for the surface wave, and the other two are for the thermocapillary instabilities, presented in §4.4. They indicated that both the hydrodynamic surface wave and the thermocapillary instability of the long wave depend strongly upon the angle of inclination of the plane.

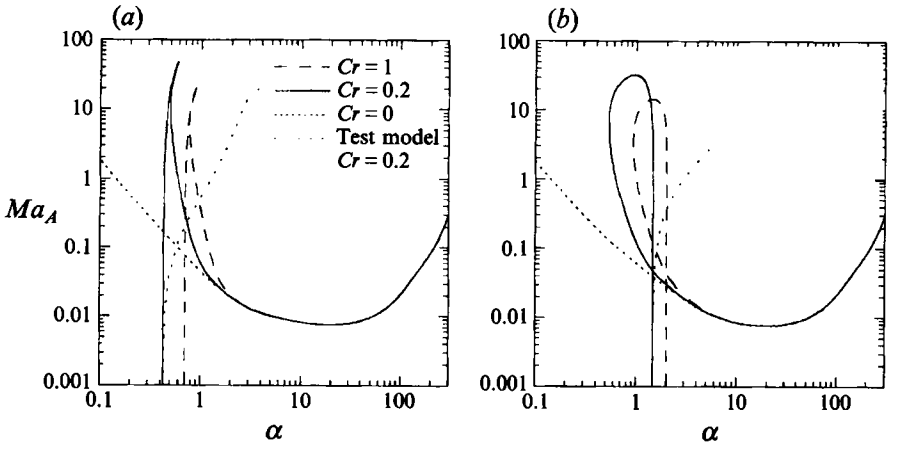

FIGURE 15. Neutral curves for the surface wave and the 'diffusion wave' at (*a*) $Re = 1$ and (*b*) $Re = 100$ in the case of $\Gamma = 0$ ($Bi_A = 10, Pe_A = 10^6$).

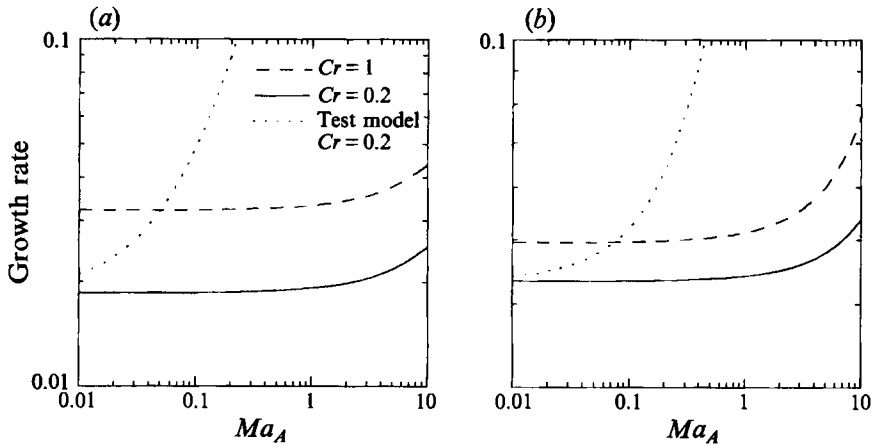

FIGURE 16. Maximum growth rate of the surface wave in the case of $\Gamma = 0$, for (*a*) $Re = 1$ and (*b*) $Re = 100$ ($Bi_A = 10, Pe_A = 10^6$).

Their result showed that on increasing the angle, the range of values of the Archimedes number (which measures the depth of the layer) for which the flow is stable decreases. The two unstable regions in the diagram may then form a single unstable region for certain large angles. In the limit case of a vertical falling film, the hydrodynamic surface wave is unstable for all depths (Benjamin 1957; Yih 1963).

In our stability diagrams for a vertical falling film in the presence of a surfactant, it appears that there could be only one unstable region for large-wavelength disturbances, although there are two mechanisms to trigger the instabilities: the basic flow shear stress and the surface tension force. It therefore may not be possible to show the Marangoni instability of the interfacial mode explicitly here, but, at least, we may determine how the two mechanisms affect each other in causing the instabilities in the region of small wavenumbers.

Results in §4.3 show that the presence of a surface-active solute stabilizes the surface wave, see figure 8. The stabilizing effect is largely due to adsorption of the surfactant, the parameter Γ, see figure 9. In order to compare our results with the previous works,

we need to recalculate the surface wave for zero surface-excess concentration ($\Gamma = 0$). In addition to this, there is an another difference between our model and that of Goussis & Kelly (1991): the surface tension in the normal force balance, expressed by the sum of the two terms in the second square brackets of (30), increases with the Marangoni number Ma_A in the present model but it is fixed in theirs. We shall remove the term multiplied by Ma_A in (30) in the following calculations.

Figures 15(*a*) and 15(*b*) show the neutral curves for both the surface wave and the 'diffusion wave' in the (Ma_A, α)-plane using Cr as a parameter, for $Re = 1$ and 100 respectively. Figures 16(*a*) and 16(*b*) show the maximum growth rates as a function of the Marangoni number, again using Cr as a parameter but for the surface wave only. We also examine here a special case where the effect of the surfactant on the flow is only due to the modification of the basic concentration at the free surface by the surface deformation, the perturbed concentration not being considered, i.e. the last term on the left of (31) being removed. There is no unstable 'diffusion wave' in this special case. The results marked 'Test model' in the figures, show clearly that the two mechanisms – the basic flow shear stress and the surface tension force – reinforce each other in causing instabilities in the region of small wavenumbers, both the critical wavenumbers and the growth rates of the surface wave increasing gradually with increasing Ma_A. This is in accordance with the results of previous authors (Goussis & Kelly 1991). However, the critical wavenumbers and the growth rates increase only slightly when the perturbed concentration is present in (31), for both $Cr = 1$ and 0.2. This demonstrates that the mechanism which could cause an unstable 'diffusion wave' stabilizes the instabilities of long-wave disturbances. In the case of $Cr = 0$ there is only a 'diffusion wave', because the deformation of the free surface ($Cr \neq 0$) is essential for both mechanisms which may trigger the surface wave and the Marangoni instability of the interfacial mode respectively.

There would be only one unstable region for the surface wave and the 'diffusion wave' in the (Ma_A, α)-plane when the Marangoni number is large enough, see figures 15(*a*) and 15(*b*). The value of Ma_A above which the two unstable regions merge decreases as Cr increases. These may be analogous to the results reported by Goussis & Kelly (1990) in their stability diagrams: the two unstable regions for the thermocapillary instabilities approach each other as the Marangoni number increases for large Bond numbers (which is equivalent to Cr in measuring surface tension), forming a single unstable region.

Figures 15(*a*) and 15(*b*) also show that with increasing Cr the unstable region for surface wave increases, while the unstable region for the 'diffusion wave' decreases for small wavenumbers. This seems to be in conflict with the previous results that the surface deformation destabilizes the Marangoni instabilities (Scriven & Sternling 1964; Goussis & Kelly 1990). However, one may note that the Marangoni instability studied here is for transverse waves whose wave number vectors are in the direction of film flow. Goussis & Kelly (1991) indicated that there is stabilizing effect from the basic flow on the Marangoni instability of the transverse waves due to the basic shear stress at the free surface and the Reynolds stress in the bulk of the fluid. The results of figures 15(*a*) and 15(*b*) may then be understood as follows. For small wavenumbers, a higher Cr (or a lower surface tension) will result in a larger surface deformation, and thus cause a more unstable surface wave. But it may not necessarily destabilize the 'diffusion wave' since the stabilizing effect from the basic flow would be larger for a larger surface deformation. Consequently, the 'diffusion wave' may be more stable for a lower surface tension. For large wavenumbers, the surface tension effect becomes stronger in opposing the surface deformation. The stabilizing effect from the basic flow due to the

surface deformation then becomes smaller, tending to being negligible. The neutral curves are then almost independent of the Crispation number. Numerical results indicate that for very large wavenumbers the critical Ma_A in figure 15 actually decreases as Cr increases, though the decreases are too small to be seen from the figure.

Results of this subsection, calculated for the case of $\Gamma = 0$, demonstrate the Marangoni instability for large-wavelength disturbances. However, the instability is stabilized by the perturbed concentration at the interface. In the case of $\Gamma \neq 0$, the instability may be completely suppressed, like the results shown in previous sections.

5. Conclusions

In Li & Ji (1994), a linear stability analysis of a falling film yielded the previously known surface wave mode of instability and a mode which was called the 'wall wave' mode. Performing the same analysis for a film with a surface-active solute here, we found an additional mode of instability at low Reynolds number. This conditionally unstable mode originates in the eigen-equation for the advection–diffusion of the solute, and it is therefore called 'diffusion wave' here. The corresponding unstable wave is thought of as induced by the Marangoni effect.

As found by earlier authors, the presence of a surface-active solute stabilizes the surface wave. The growth rate and the wavenumber for the most unstable wave as well as the critical wavenumber all decrease. But the wave velocity for the most unstable wave increases.

Introducing a surfactant has a negligibly small effect on the 'wall wave' mode of instability, which is easily understood: the 'wall wave' mode is mainly associated with the wall but the effect of a surfactant is largely near the interface.

Whether the 'diffusion wave' will be stable or unstable depends on several parameters. The onset of instability is favoured by a large Marangoni number, a low adsorption number and a large Biot number or, in physical terms, the faster the solute evaporates, the less adsorbed it is, the more unstable the mode will be. However, the 'diffusion wave' may never become unstable for small Ma_A or Bi_A, or large Γ depending on the Reynolds number. The volatile property of the surfactant in the model is necessary to cause the Marangoni instability of the 'diffusion wave' because it produces a non-uniform profile of the basic concentration. The unstable 'diffusion wave' occurs preferably for low Reynolds numbers, and it has higher wavenumber (or shorter wavelength) in comparison with the surface wave.

The Marangoni instability of the 'diffusion wave' is thought to be analogous to the thermocapillary instability examined first by Pearson (1958) for a thin layer of fluid heated from below. The Marangoni instability of large-wavelength disturbances, revealed recently by Goussis & Kelly (1990) in a study of the same system as Pearson's but allowing surface deformation, is examined for present system as well, assuming a zero surface-excess concentration of the surfactant. However, when adsorption is considered, the Marangoni instability of the interfacial mode may be completely suppressed.

As mentioned in the Introduction, it has been found that surface-active agents could increase the capacity of absorption cooling machines. One conjecture to explain the phenomenon is that the surfactants could improve the mass transfer in the falling films of the absorber of the machines. The results of the present work may provide a confirmation of the conjecture as follows. The instability of a falling film without surfactants at low or moderate Reynolds numbers is governed by the surface wave mode. This mode is unstable for large-wavelength disturbances. The Marangoni effect

in the presence of a surfactant leads to the unstable 'diffusion wave' for moderate- or small-wavelength disturbances. This 'diffusion wave', which may attach to the long surface wave, could enhance the mass transfer rate of an absorption falling film. However, this work could only provide a qualitative explanation: the absorption process which includes both heat and mass transfer has not been considered in the present model, and the Marangoni instabilities of longitudinal rolls, which may be more unstable than the instabilities of transverse waves (Goussis & Kelly 1991), have not been examined.

The authors wish to thank Dr J. Li for his useful suggestions in the solution method for the eigenvalue problem. The authors wish also to thank Dr H. Bjurström for helpful discussions. Many useful criticisms by the referees are gratefully acknowledged.

Appendix. Unperturbed concentration profile for the surface-active solute

In the steady unperturbed state, the velocity field has been assumed to be one-dimensional, as in equation (1): $U = 1-y^2$ and $v = 0$. Substituting (12) into (4), (9) and (11), using the one-dimensional velocity, we obtain the dimensionless equations for the unperturbed concentration of the surfactant,

$$U\frac{\partial c_A}{\partial x} = \frac{1}{Pe_A}\left(\frac{\partial^2 c_A}{\partial x^2}+\frac{\partial^2 c_A}{\partial y^2}\right), \tag{A 1}$$

with boundary conditions

$$\frac{\partial c_A}{\partial y} = Bi_A c_A \quad \text{at} \quad y = 0, \tag{A 2}$$

$$\frac{\partial c_A}{\partial y} = 0 \quad \text{at} \quad y = 1, \tag{A 3}$$

where Pe_A is the mass Péclet number for the additive, and Bi_A the Biot number, defined in (15).

Since the mass Péclet number for additives Pe_A may be estimated as 10^6–10^7 (Perry & Chilton 1973), the penetration depth of the surfactant will be much smaller than the depth of the film for the contact times of the film with the gas phase in practical cases. We may then assume $U = 1$ when solving (A 1) and neglect the diffusion in the x-direction in comparison with that in the y-direction. Using a semi-infinite-layer approximation, and assuming that the concentration of c_A^* is c_{A_0} at the initial $x^* = 0$, or in dimensionless form: $c_A = 1$ at $x = 0$, a solution can be obtained by the Laplace transform technique as follows:

$$c_A(x,y) = \operatorname{erf}(y_1)+\exp(g^2-y_1^2)\,[1-\operatorname{erf}(g)], \tag{A 4}$$

with

$$y_1 = \frac{y}{2(x/Pe_A)^{1/2}}, \quad g = y_1 + Bi_A\,(x/Pe_A)^{1/2},$$

where erf is the Error function. The concentration profile depends on both x and y. However, for large values of Pe_A, the dependence of the unperturbed concentration (A 4) on x may be quite weak. In the stability analysis, we may assume that the concentration of the surfactant at the basic state is a function of y only.

REFERENCES

BENJAMIN, T. B. 1957 Wave formation in laminar flow down an inclined plane. *J. Fluid Mech.* **2**, 554.

BOURNE, J. R. & EISBERG, K. V. 1966 Maintaining the effectiveness of an additive in absorption refrigeration systems. *US Patent* 3 276 217.

BRIAN, P. L. T. 1971 Effect of Gibbs adsorption on Marangoni instability. *AIChE J.* **17**, 765.

BRIAN, P. L. T. & ROSS, J. R. 1972 The effect of Gibbs adsorption on Marangoni instability in penetration mass transfer. *AIChE J.* **18**, 582.

CASTILLO, J. L. & VELARDE, M. G. 1985 Marangoni convection in liquid films with a deformable open surface. *J. Colloid Interface Sci.* **108**, 264.

DIJKSTRA, H. A. 1988 Mass transfer induced convection near gas–liquid interfaces. Ph.D. thesis, Groningen.

EMMERT, R. E. & PIGFORD, R. L. 1954 A study of gas absorption in falling liquid films. *Chem. Engng Prog.* **50**, 87.

GOUSSIS, D. A. & KELLY, R. E. 1990 On the thermocapillary instabilities in a liquid layer heated from below. *Intl J. Heat Mass Transfer* **33**, 2237.

GOUSSIS, D. A. & KELLY, R. E. 1991 Surface wave and thermocapillary instabilities in a liquid film flow. *J. Fluid Mech.* **223**, 25.

HO, K. & CHANG, H. 1988 On nonlinear doubly-diffusive Marangoni instability. *AIChE J.* **34**, 705.

IMAISHI, N., HOZAWA, M., FUJINAWA, K. & SUZUKI Y. 1983 Theoretical study of interfacial turbulence in gas–liquid mass transfer, applying Brian's linear-stability analysis and using numerical analysis of unsteady Marangoni convection. *Int. Chem. Engng* **23**, 466.

JI, W., BJURSTRÖM, H. & SETTERWALL, F. 1993 A study of the mechanism for the effect of heat transfer additives in an absorption system. *J. Colloid Interface Sci.* **160**, 127–140.

KASHIWAGI, T., KUROSAKI, Y. & SHISHIDO, H. 1985 Enhancement of vapour absorption into a solution using the Marangoni effect. *Nihon Kikai Gakkai Ronbunshu* **B 51**, p. 1002.

KASHIWAGI, T., WATANABE, H., OMATA, K. & LEE, D. H. 1988 Marangoni effect in the process of steam absorption into the falling film of the aqueous solution of LiBr. *KSME-JSME Thermal and Fluid Eng. Conf., Seoul, Korea.*

KELLY, R. E., DAVIES, S. H. & GOUSSIS, D. A. 1986 On the instability of heated film flow with variable surface tension. *Heat Transfer 1986: Proc. 9th Intl Heat Transfer Conf., San Francisco*, vol. 4, p. 1936.

LI, J. & JI, W. 1994 A tridiagonal solver for the Orr–Sommerfeld equation. *Intl J. Numer. Meth. Fluids* (submitted).

LIN, S. P. 1970 Stabilizing effects of surface-active agents on a film flow. *AIChE J.* **16**, 375.

LIN, S. P. 1975 Stability of liquid flow down a heated inclined plane. *Lett. Heat Mass Transfer* **2**, 361.

MCTAGGART, C. L. 1983 Convection driven by concentration- and temperature-dependent surface tension. *J. Fluid Mech.* **134**, 301.

PEARSON, J. R. A. 1958 On convection cells induced by surface tension. *J. Fluid Mech.* **4**, 489.

PÉREZ-GARCIA, C. & CARNEIRO, G. 1991 Linear stability analysis of Bénard-Marangoni convection in fluids with a deformable free surface. *Phys. Fluids* **A 3**, 292.

PERRY, R. H. & CHILTON, C. H. 1973 *Chemical Engineers' Handbook*, 5th Edn, pp. 3–224. McGraw-Hill.

SCRIVEN, L. E. & STERNLING, C. V. 1964 On cellular convection driven by surface-tension gradients: effects of mean surface tension and surface viscosity. *J. Fluid Mech.* **19**, 321.

WHITAKER, S. 1964 Effect of surface active agents on the stability of falling liquid films. *Indust. Engng Chem. Fundam. Q.* **3**, 132.

WHITAKER, S. & JONES, L. O. 1966 Stability of falling liquid films. Effect of interface and interfacial mass transport. *AIChE J.* **12**, 421.

YAO, W., BJURSTRÖM, H. & SETTERWALL, F. 1991 Surface tension of lithium bromide solutions with heat-transfer additives. *J. Chem. Engng Data* **36**, 96.

YIH, C. S. 1963 Stability of liquid flow down an inclined plane. *Phys. Fluids* **6**, 321.